

Article

# Miniaturized Blood Pressure Telemetry System with RFID Interface

Michele Caldara <sup>1</sup>, Benedetta Nodari <sup>1,\*</sup>, Valerio Re <sup>1</sup> and Barbara Bonandrini <sup>2</sup>

<sup>1</sup> Department of Engineering, University of Bergamo, Viale Marconi 5, Dalmine (BG) 24044, Italy; michele.caldara@unibg.it (M.C.); valerio.re@unibg.it (V.R.)

<sup>2</sup> Istituto di Ricerche Farmacologiche “Mario Negri”, Via Stezzano 87, Bergamo 24126, Italy; barbara.bonandrini@marionegri.it

\* Correspondence: benedetta.nodari@unibg.it; Tel.: +39-035-205-2159

Academic Editors: Enzo Pasquale Scilingo and Gaetano Valenza

Received: 23 May 2016; Accepted: 22 August 2016; Published: 30 August 2016

**Abstract:** This work deals with the development and characterization of a potentially implantable blood pressure telemetry system, based on an active Radio-Frequency IDentification (RFID) tag, International Organization for Standardization (ISO) 15693 compliant. This approach aims to continuously measure the average, systolic and diastolic blood pressure of the small/medium animals. The measured pressure wave undergoes embedded processing and results are stored onboard in a non-volatile memory, providing the data under interrogation by an external RFID reader. In order to extend battery lifetime, RFID energy harvesting has been investigated. The paper presents the experimental characterization in a laboratory and preliminary in-vivo tests. The device is a prototype mainly intended, in a future engineered version, for monitoring freely moving test animals for pharmaceutical research and drug safety assessment purposes, but it could have multiple uses in environmental and industrial applications.

**Keywords:** blood; embedded; energy harvesting; implantable; in-vivo; ISO 15693; low-power; pressure; RFID

## 1. Introduction

In recent years, implantable smart sensors and Wireless Sensor Network (WSN) technologies have been considered key research areas for both computer science and electronics. Reliable physiological parameters monitoring with miniaturized smart sensor nodes can enhance healthcare applications and, at the same time, to improve the patient quality of life. Implantable telemetry systems take advantage of continuous electronic components miniaturization, progresses in sensor capability, diffusion of wireless data transfer technologies and power consumption reduction. The synergy between Micro Electro-Mechanical Systems (MEMS), a microcontroller and RFID technologies allows to extend the sensor capabilities by adding embedded computational power and wireless interface with the lowest possible supply consumption, enabling in this way the achievement of accurate and low-cost wireless systems. Telemetry is a well-established method of monitoring physiological functions in awake and freely moving laboratory animals, while minimizing stress artifacts. Currently, such systems are employed in pharmacological research to measure physiological signals such as blood pressure, heart rate, blood flow, electrocardiogram, respiratory rate, sympathetic nerve activity, body temperature etc., in a wide range of animal species: small animals such as rats, mice, gerbils and hamsters; and medium animals, such as dogs, rabbits, monkeys, guinea pigs, and pigs, etc. [1]. Nowadays, the small size of implantable monitoring devices and their extended battery lifetime permit in-vivo tests for several days, with no necessity of manipulation, leading to an improvement of experiments capabilities [2]. Most of animal implantable telemetry systems are composed by a small biocompatible enclosure containing

the sensor, the electronic device and the battery plugged to a catheter filled with physiological solution. The catheter end is inserted into an artery and it is fixed with biocompatible glue. The commercial systems are usually designed to accommodate intraperitoneal placement. Typically, the animal cage is placed near the system receiver for allowing data transmission. The main wireless technologies for transmitting data are definitely Bluetooth, Wi-Fi, General Packet Radio Service, Enhanced Data rates for Gsm Evolution, ZigBee and Near Field Communication (NFC). NFC protocols are developed on the radiofrequency identification RFID standards, in particular exploiting the industrial, scientific and medical (ISM) radio band at  $13.56 \text{ MHz} \pm 7 \text{ kHz}$ , which is worldwide available. Nowadays, the use of the RFID in telemetry and telemedicine is increasing considerably in the biomedical and health domains. This is due to the fact that the solutions for human and animal implants are advantageous in terms of exposure to Electro Magnetic fields, since in the range 1–20 MHz human tissues do not significantly attenuate the electromagnetic waves. Moreover, the external reader provides the power needed to establish the communication [3]. The system disclosed in this paper is an active RFID sensing tag, compliant with the ISO 15,693 protocol, capable to continuously measure and process the arterial blood pressure data, providing results to an external reader. The electronics are intended to be placed in a subcutaneous region of small/medium animals, with the goal of achieving a minimal invasive implant and of reducing the tag-reader distance. The paper describes the system in terms of hardware and firmware, the laboratory characterization and preliminary in-vivo test. Long-term animal studies will be performed with the next version of the system, after further miniaturization and proper encapsulation.

## 2. RFID Pressure Sensing System

### 2.1. Requirements

The aim of such a work is to develop a prototype capable to continuously monitoring blood pressure, with the requirement to be comparable to the state-of-the-art in terms of dimensions and functionalities. For this reason, the device specifications have been dictated by state-of-the-art implantable systems, whose main features are summarized in Table 1. The system, based on Near Field Communication (NFC) technology and embedded processing, has been conceived in order to be potentially implantable in test animals (rats), used in pharmaceutical research field and human [2]. It requires only a revision of the electronics toward further miniaturization.

**Table 1.** State-of-the-art of telemetry system for small animals and human.

Sensor	Use	Sensor Dimensions	Range	Resolution & Accuracy
DataSCI (HD-S21)	Blood pressure (small animals)	5.9 cc; 8 gr;	−20–300 mmHg	$\pm 3 \text{ mmHg}$ ; −0.25 mmHg/month;
TSE (Stellar)	Blood pressure (small animals)	6 cc; 11 gr; 16 × 30 mm <sup>2</sup> ;	0–300 mmHg	-
Millar (TRM54P)	Blood pressure (small animals)	12 gr;	−20–300 mmHg	$\pm 2 \text{ mmHg}$ ; <4 mmHg/month
Mitter (G2 HR)	Heart rate (small animals)	11 gr; 15.5 × 6.5 mm <sup>2</sup> ;	120–780 BPM	1.5%
<i>Developed system</i>	Blood pressure (small animals)	8 gr; 5.6cc; 30 × 17.5 × 11 mm <sup>3</sup>	0–300 mmHg	$\pm 3 \text{ mmHg}$ ;
ENDOCOM	Blood pressure (Human)	15 × 18.5 mm <sup>2</sup>	-	-
Cardio MEMS	Blood pressure (Human)	2 × 3.4 × 15 mm <sup>3</sup>	-	-

The device main requirements concern the small volume (in the range 4.4–6 cm<sup>3</sup>), the weight (in the range 7.6–12 gr), the pressure accuracy ( $\pm 3 \text{ mmHg}$ ) and the capability of continuously measuring blood pressure in the range 0–300 mmHg. For an accurate determination of the maximum and the minimum pressure values, considering that the maximum heart rate of rats can be up to 400 bpm (6.67 Hz), the pressure signal should be sampled at least a factor ten of the maximum rat's

heart rate (i.e., 66.67 Hz). This permits a good reconstruction of the pressure wave after acquisition and to better identify the minimum and maximum values. Moreover, the typical experiment duration in pharmacological research is about 10 days, implying ultra-low power electronics, which permit the use of a small and lightweight battery. In order to have an efficient and optimal system, the blood pressure wave is measured and processed on-board, thus only the maximum and minimum values are stored on a local memory of the device, leaving the freedom of a subsequent data upload via RFID, without the risk of losing acquired data. Despite this, if required, the device is able to transmit the full waveform data. The embedded processing can open new approaches in conducting experiments, minimizing the data transfer time and better exploiting the local memory usage.

## 2.2. Sensor Platform Description

The architecture of the system is depicted in Figure 1a. The pressure sensor is coupled to a catheter, filled with biocompatible saline solution, with the purpose to sense the blood pressure signal once it is inserted into an artery. In order to prevent the clots inside the catheter, the saline solution could be mixed with anticoagulant. The pressure is thus transferred to the opposite end of the catheter where the pressure sensor membrane is placed. An ultra-low-power microcontroller processes instantaneous pressure data and it stores the results on a non-volatile memory. The board bill of material, minimized to reduce area occupancy, includes the pressure sensor, the low-power microcontroller (STM32L162RD, STMicroelectronics, Geneva, CH, Switzerland), a non-volatile memory (M24LR64E-R EEPROM 64 kbit, STMicroelectronics) with a double interface (I2C and RFID), and an energy harvesting pin. The latter being capable of providing microcontroller analysis results via RFID. The system includes also an optimized power management chain and a Li-poly rechargeable battery to power the device (PWB1389). Thanks to the electronic device's low power-consumption, the battery capacity is only 90 mAh, with volume of only  $25 \times 11 \times 3.5 \text{ mm}^3$  and an approximate weight of 2 gr. While the battery voltage decreases from 4.1 V to 3 V during the procedure, the buck boost regulator is able to maintain a constant supply value of 3.4 V. Cascaded to the buck boost, a dedicated Low DropOut regulator (LDO) is used to supply the sensor and the Electrically Erasable Programmable Read-Only Memory (EEPROM) at 3.3 V only when a measurement or memory communication is needed, additionally providing a noiseless supply for the sensors.

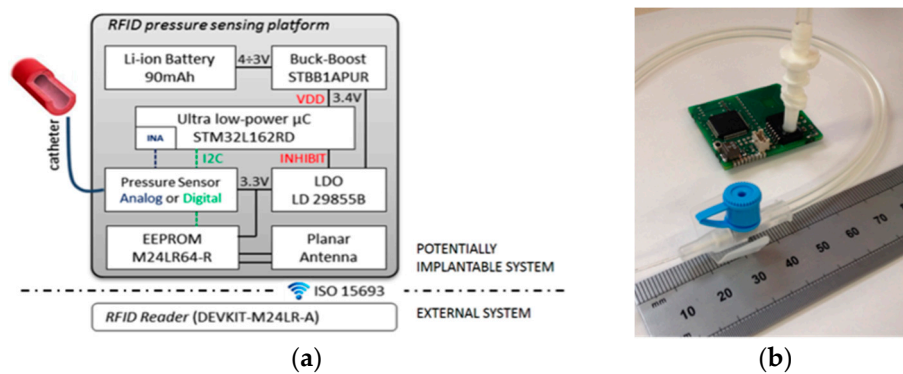


**Figure 1.** (a) Sensor platform block diagram. The potentially implantable system is above the dotted line; (b) Laboratory setup for characterization; vertically stacked mechanical arrangement suitable for implant.

The developed device, depicted in Figure 1b, is assembled on a two layers  $34 \times 30 \text{ mm}^2$  FR4 (Flame Retardant 4) printed circuit board, designed in order to be divided in two parts, which can be stacked vertically with the battery. Such a configuration creates a “multilayer” system with total dimension of  $30 \times 17.5 \times 11 \text{ mm}^3$ , a volume of  $5.6 \text{ cm}^3$  and a weight of 8 gr. Such compactness is comparable with some of the most diffused telemetering systems cited in Table 1 and it makes the system potentially implantable in the abdominal cavity of the animal, once coated with a biocompatible

material. By replacing an actual components case with smaller packages it can dramatically reduce the present device volume, with a minimal impact on the cost. The choice of the actual components case has been dictated by the need of test and debugging. In order to further reduce the device volume and to improve robustness, the interconnection between the catheter and the sensor should also be improved. The Printed Circuit Board (PCB) has been designed with the capability of alternatively mounting two different temperature-compensated pressure sensors. The first one is analog (MPX2300DT1, Freescale, Austin, TX, USA) and the second one is digital (NPA-700M-005D, General Electric, Fairfield, CT, USA), both selected for their pressure accuracy of  $\pm 3$  mmHg in the range 0–260 mmHg. Table 2 summarizes the main features of both sensors; they have been characterized experimentally with the purpose of determining the optimal solution in terms of power consumption and resolution.

**Table 2.** Digital and analog pressure sensor main features.

Features	Digital Sensor	Analog Sensor
Pressure range	0–260 mmHg	0–300 mmHg
Dimension	$9 \times 11$ mm <sup>2</sup>	$9 \times 6$ mm <sup>2</sup>
Sensitivity	50 counts/mmHg	$5 \mu\text{V}/\text{V}/\text{mmHg}$
Accuracy	$\pm 1.5\%$	$\pm 1.5\%$
Interface	I2C	Analog differential
Max ODR *	833 Hz	ADC ** sample rate
Supply current (at 10 V)	1.5 mA	1 mA

\* Output Data Rate; \*\* Analog to Digital Conversion.

The RFID reader (DEVKIT-M24LR-A, STMicroelectronics) is placed under the cage of the animal and it provides the features summarized in Table 3.

**Table 3.** RFID reader main features.

Features	DEVKIT-M24LR-A
Antenna dimensions	$337 \times 237$ mm <sup>2</sup>
Operating frequency	13.56 MHz
Max transmitting power	1 W
Interface	I2C and RF

### 2.3. Firmware

Typically the drug assessment experiments need to monitor the arterial blood pressure every minute for several days, so it is not needed to monitor each cardiac cycle. For this reason, the firmware has been implemented in such a way that the microcontroller acquires pressure sensor data for 5 s. Then it applies an algorithm for the maximum and minimum detection and computes the average systolic and diastolic pressure values. Finally, the microcontroller stores the results on the non-volatile memory. The LDO which provides a supply for the sensor and the EEPROM is disabled until the next acquisition occurs. After this phase, in order to maximize the device operation time, the microcontroller enters into a stand-by mode for 55 s and successively it wakes-up thanks to the internal real-time clock (RTC). Since the EEPROM collects all the data permanently, it is not necessary to have an active communication link between the sensor and the RFID reader for all the experiment duration. When the external reader identifies the tag memory, all the data history is downloaded and erased for the next acquisitions.

The system embedded firmware includes the algorithm for the identification of the blood pressure peaks, essential for analyzing the effects of pharmacological treatments on test animals. Peaks and troughs, corresponding to systolic and diastolic pressure respectively, characterize the blood pressure signal. Systolic phase occurs during ventricles contraction, while diastolic phase take places at the beginning of the cardiac cycle, when the ventricles are filled. The identification of peaks is a

common problem in the analysis of physiological signals; often it is necessary to detect peaks in real time, but the task is frequently complicated by baseline wander and other type of interference [4]. The search for systolic and diastolic pressure of every cardiac cycle has been implemented with the Todd-Andrews algorithm. The choice of such an algorithm is due to the benefits in terms of local peaks, baseline wandering and dynamic threshold immunity. It mainly consists of three steps: First, it looks for the maximum on the rising edge of the signal by comparing each sample in the array with the previous one. Then it calculates the difference between every sample of the falling edge and the identified maximum. If the result of the subtraction is greater than a fixed threshold, the global maximum has been found. The threshold can be computed dynamically on the amplitude of the previous signal period. The same process is applied on the falling edge to find the minimum value. Figure 2 shows the algorithm validation that has been done manually varying the input signal pressure with a sphygmomanometer.

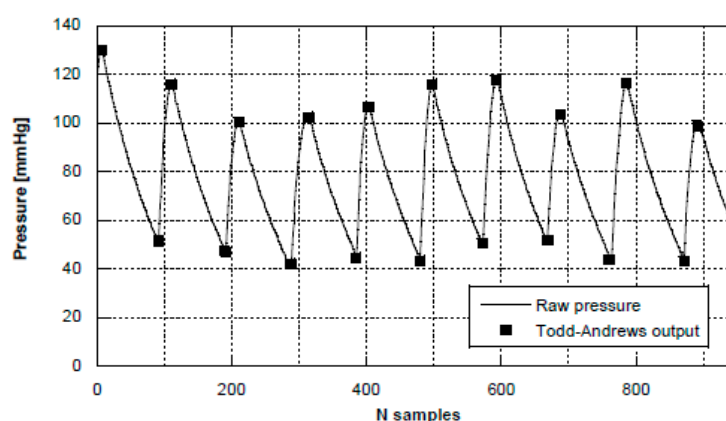


**Figure 2.** Algorithm validation, performed varying pressure and representing raw data, obtained from the digital pressure sensor and algorithm max/min determined values.

#### 2.4. Power Consumption

The device's power consumption has been characterized on each component at different operating modalities by replacing the battery with a power supply (Agilent E363A, Santa Clara, CA, USA), remotely controlled in order to track the sourced current. The battery lifetime is approximately 67 h for the system using digital sensor and about 63 h with the analog sensor. The difference between them is given by the power consumption of the microcontroller ADC needed only for analog sensor signal acquisition (see Table 4). In order to satisfy the specification of a 10 day lifetime, it turns out to power the device with a Li-poly battery with an increased capacity (300 mAh could be suitable) or to take advantage of the EEPROM energy harvesting function, that it has been characterized in a following paragraph. The current consumption of 0.7 mA during system stand-by mode is only due to the voltage regulator quiescent current and RTC clock activated.

**Table 4.** Device supply currents.

Pressure Sensor Mounted	Average Current Provided by the Battery ( $V = 3.7\text{ V}$ )			
	I <sub>run</sub> ( $\Delta T = 5\text{ s}$ )		I <sub>sleep</sub> ( $\Delta T = 55\text{ s}$ )	I <sub>average</sub> ( $\Delta T = 60\text{ s}$ )
	I <sub>sensor + EEPROM</sub>	I <sub>total</sub>		
Analog	3.41 mA	9.49 mA	0.7 mA	1.43 mA
Digital	3.53 mA	8.51 mA	0.7 mA	1.35 mA

### 2.5. The RFID Interface

RFID technology for human and animal implants is generally based on passive or active devices and makes it possible to achieve read ranges in the order of 10 s of centimeters, a very short range once compared to the other wireless technologies, but suitable to the majority of the applications. Basically, an RFID interface uses communication via electromagnetic waves to exchange data between an interrogator (also known as the reader) and an object (transponder or tag). The communication must respect given standards, as the protocol ISO 15693, in which the 13.56 MHz carrier electromagnetic wave is ASK (Amplitude Shift Keying) modulated for data transmission [5,6]. ASK wave is 10% or 100% modulated, obtaining a data rate of 1.6 kbps using the 1/256 pulse coding mode or a maximum data rate of 26 kbps using the 1/4 pulse coding mode. An integrated circuit for storing and processing data and an antenna for receiving and transmitting them, generally compose the transponder. The electromagnetic field generated by the interrogator provides the power to the transponder for the data communication, achieving a wireless link with no power consumption on the transponder side. Unlike other wireless technologies, the obtainable data rate is quite limited, suggesting a one-shot measurement operation or an on-board data processing in order to optimize the transmission time. From the review of state-of-the-art RFID devices, it can be observed that inductive coupling operating in HF (13.56 MHz and below) frequency range is presently the best method to wirelessly send power and data from off-body interrogator to RFID device implanted inside body. Since in the range 1–20 MHz the EM waves are not significantly attenuated by human tissues [7,8].

The width of the PCB has been constrained by the size of the antenna, designed with a square shape as a two layers planar coil on the PCB. In fact, to allow the implantable system to interact with the external reader through RFID communication, the antenna should have an outer diameter of 15.7 mm and an internal one of 5.1 mm. Moreover, considering the spacing and width of the convolutions of 10 mils, the antenna should have 12 turns [9]. The shape and the dimensions used for the antenna allow also to obtain a value of a measured self-inductance equal to 4.6  $\mu\text{H}$  (4.7  $\mu\text{H}$  theoretical), in order to have a resonant circuit at 13.56 MHz. The RFID antenna self-inductance has been measured with an Impedance Analyzer (Agilent 4395A, Santa Clara, CA, USA) on a frequency span up to 500 MHz (see Figure 3). A self-resonance at 36 MHz, due to the antenna parasitic capacitance (4 pF), is clearly visible in Figure 3. The operating point at 13.56 MHz is also emphasized.

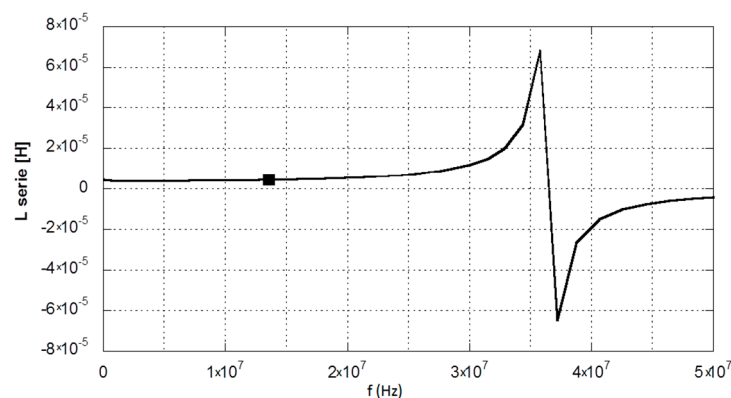


**Figure 3.** Radio Frequency Identification antenna measured self-inductance. The marker indicates the RFID operating frequency at 13.56 MHz.

### 3. System Characterization and Experimental Results

The device has been initially characterized in the laboratory and then evaluated on test rats. The system functionality tests were carried out connecting a catheter to the device pressure sensor and imposing air pressure changes with the sphygmomanometer. The pressure has been monitored with both the RFID sensor tag and a reference manometer (SICK PBS), which it has an analog



4–20 mA interface (see Figure 4). For comparison purposes the firmware was modified in order to acquire the pressure signal for 20 s and store raw data on the RFID tag memory. A software application was implemented in order to view on a PC the signal pressure, uploaded using the RFID reader. The communication distance between the interrogator and the transponder has been successfully tested up to 11 cm, which does not change interposing a hand or other material (i.e., wood, plastic, etc.) between the reader and the device [10]. In fact, thanks to RFID advantages, the tissues interposed between do not significantly attenuate the electromagnetic waves during the tag-reader communication.

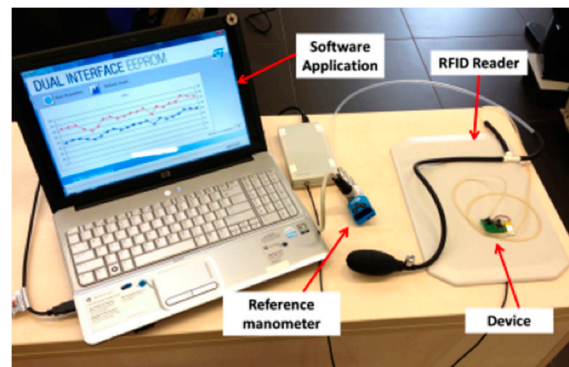


Figure 4. System setup functional sensor.

### 3.1. System with Digital Pressure Sensor

Figure 5a depicts the simultaneous acquisition of the pressure wave from the reference pressure sensor and the proposed device with digital pressure sensor mounted. The reference sensor resolution is 3 mmHg<sub>rms</sub>, whereas the device measured resolution is 2.5 mmHg<sub>rms</sub> for the digital version. The differences between the two traces are comprised between  $\pm 5$  mmHg. During the system characterization it has also been tested the maximum output data rate (833 Hz) of the I2C sensor interface, which provides a direct connection to the microcontroller.

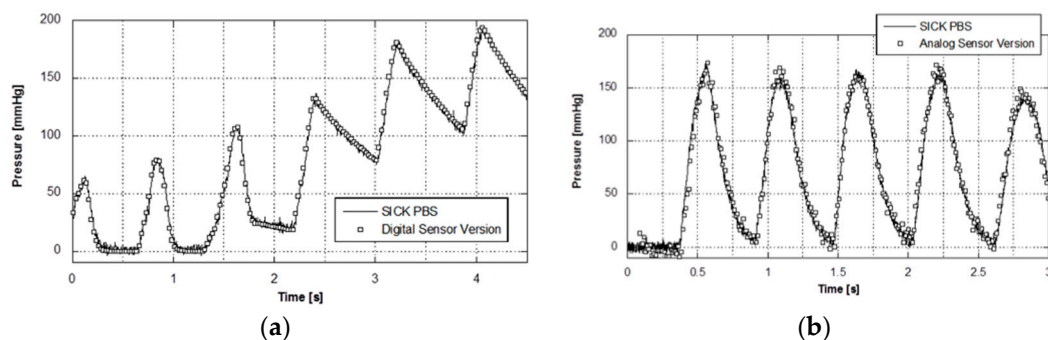


Figure 5. (a) Comparison between reference pressure sensor and the RFID tag with digital pressure sensor; (b) Comparison between reference pressure sensor and the RFID tag with analog pressure sensor.

### 3.2. System with Analog Pressure Sensor

The analog pressure sensor, based on a bridge configuration, is connected to an instrumentation amplifier (INA) obtained by using three operational amplifiers, which are embedded in the microcontroller. This solution is optimal in terms of space occupancy, since only passive elements are needed to achieve full front-end amplification. The same tests done with the digital pressure sensor have been performed even with the system with the analog sensor configuration. The measured resolution of the analog pressure sensor is 5 mmHg<sub>rms</sub> and the difference between the two acquisition traces is less than  $\pm 10$  mmHg (see Figure 5b).

Figure 6 shows the measured transfer function of the instrumentation amplifier, featuring a gain of 38.5 dB and a bandwidth of 10 kHz. The INA output is acquired by the microcontroller ADC running at 1 kS/s.

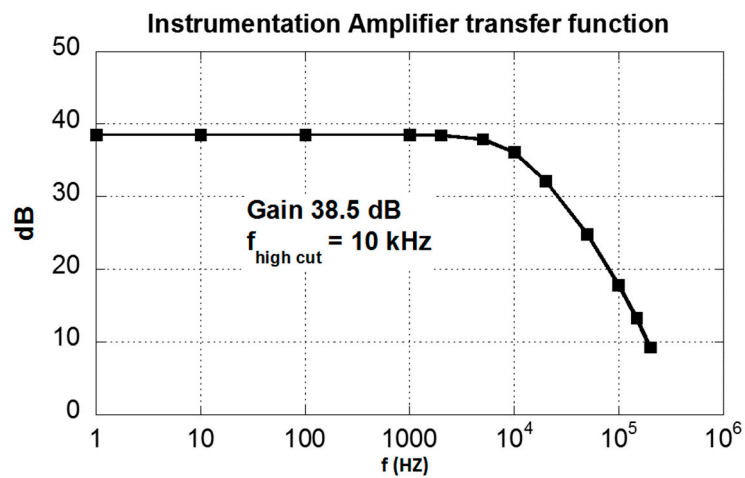


Figure 6. Instrumentation amplifier transfer function.

### 3.3. In-Vivo Tests

An adult male Sprague-Dawley rat (Charles River Laboratories International Inc., Wilmington, MA, USA) weighing 400–500 gr was used for the in-vivo tests of the proposed system, after the laboratory characterization. After anesthesia with isoflurane, the left femoral artery was isolated and cannulated with a PE50 catheter. Animal care and treatment were conducted in conformity with the institutional guidelines, in compliance with national (DL n. 116/1992, Circ. 8/1994) and international (EEC Dir. 86/609, OJL 358, Dec 1987; NIH Guide for the Care and Use of Laboratory Animals, US NRC, 1996) laws and policies. The catheter end was split and connected both to the device with digital pressure sensor mounted, placed aside the animal and to a reference pressure sensor (Deltran II, Utah Medical Products, Midvale, UT, USA), as depicted in Figure 7. The synchronous acquisitions lasting 20 s, depicted in Figure 8, are in accordance within 1 mmHg. The Fast Fourier transform of the time-base blood pressure signal is pointed out in Figure 9, showing that the blood pressure wave, having an average frequency of 5.76 Hz (346 bpm), is modulated at 0.83 Hz by the animal breath.

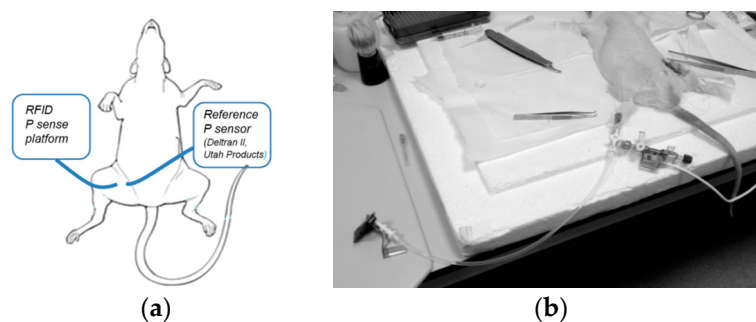
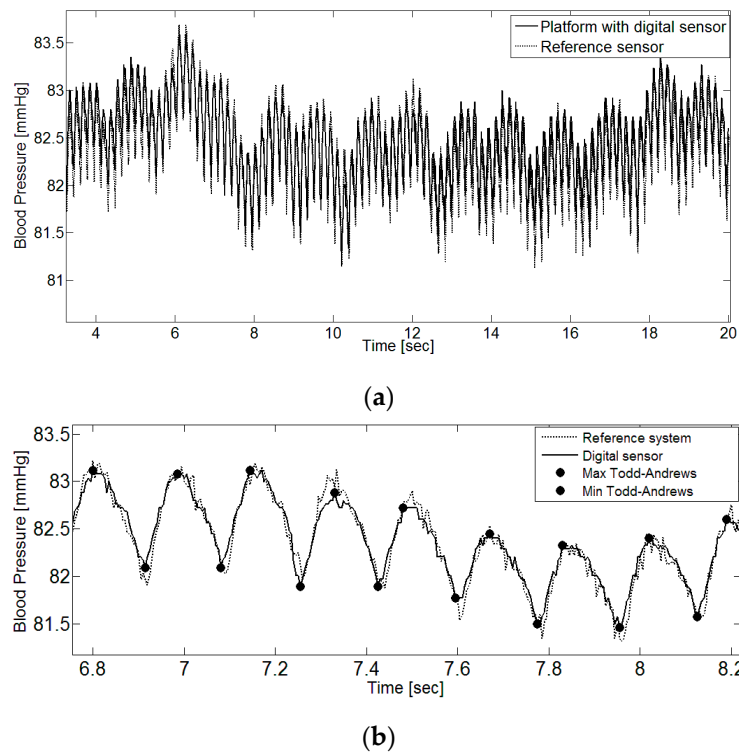
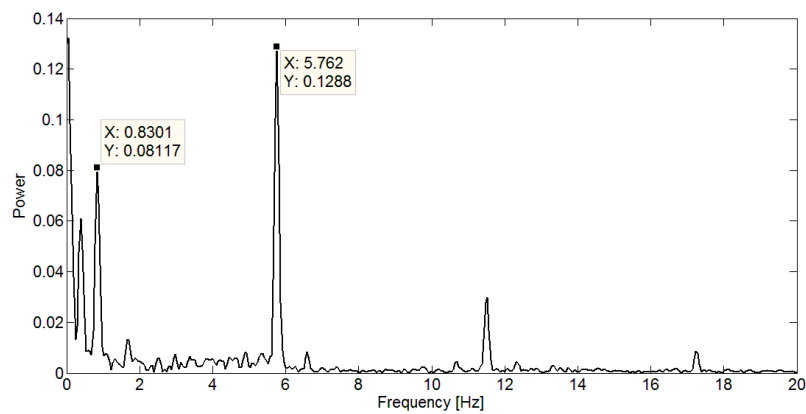


Figure 7. (a) Representation of in-vivo test set up; (b) In-vivo experiment.





**Figure 8.** (a) Synchronous recording (~20 s) of the femoral artery blood pressure with the device mounting the digital sensor and a reference measurement system; (b) zoom of the traces showing systolic and diastolic peak detection, independent of baseline wandering.



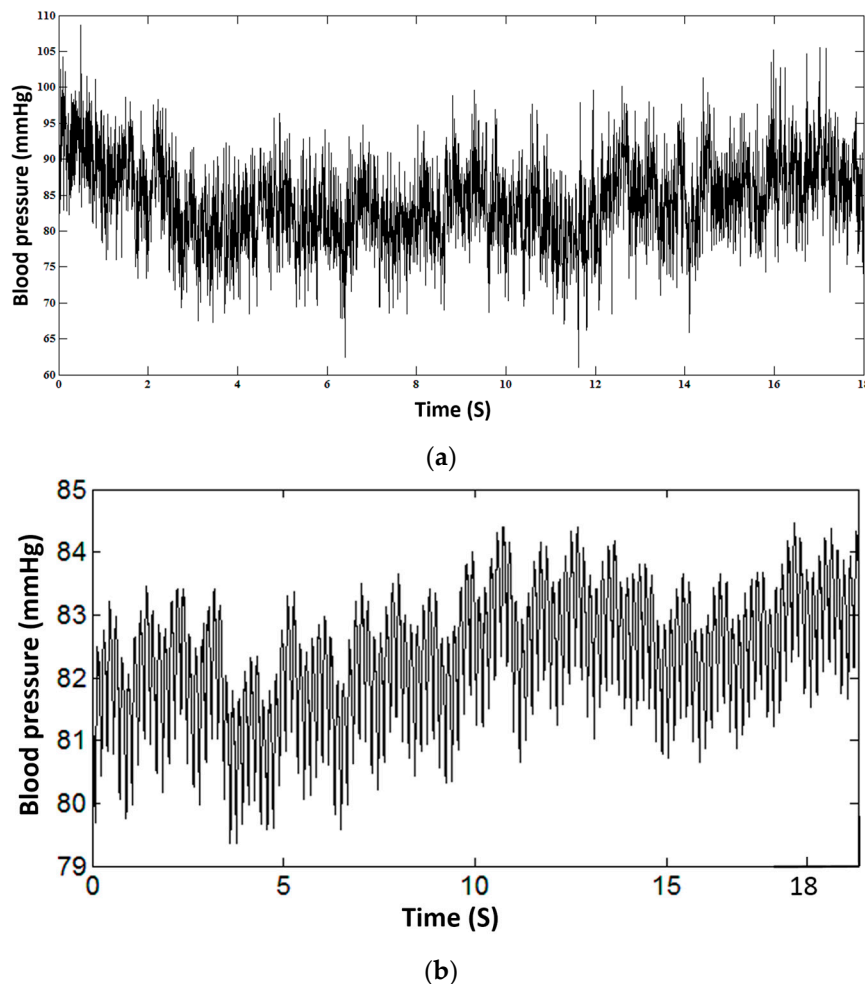
**Figure 9.** Fast Fourier transform spectrum of the signal depicted in Figure 8.

Table 5 reports the blood pressure maximum, minimum and mean values of blood pressure acquired by both the prototype and the reference sensor, during 20 s acquisition. The results obtained with the presented device are in accordance with the reference instrument within 0.12%.

**Table 5.** Maximum, minimum and mean values of blood pressure acquired by digital and reference sensor during 20 s acquisition.

Value	Digital Sensor	Reference Sensor	Error
Mean	82.57 mmHg	82.47 mmHg	0.12%
Max	83.89 mmHg	82.69 mmHg	1.43%
Min	81.14 mmHg	81.16 mmHg	0.02%

The same in-vivo test has been performed on the device mounting the analog pressure sensor, in order to compare the performances. The system was able to follow the average blood pressure but not to detect the peaks, due to its lower resolution with respect to the digital sensor version, as shown in Figure 10. The dominant frequencies in this case are not detectable as in the results obtained with the digital pressure sensor.



**Figure 10.** (a) Synchronous recording (~20 s) of the femoral artery blood pressure with the device mounting the analog sensor; (b) pressure wave acquired by the reference sensor.

### 3.4. Energy Harvesting Investigation

In order to maximize the device operation time keeping the 90 mAh small-sized battery, the EEPROM Energy Harvesting (EH) functionality has been investigated. The general purpose of the EH mode is to deliver a part of the unnecessary RF power received by the EEPROM on the RF input pin, in order to recharge the battery. When the external reader enables the EH mode and the RF field strength is sufficient, an unregulated DC voltage is provided on a pin of the EEPROM. Figure 11 shows the characterization results in terms of available power and supplied current by the EEPROM with different loads, in function of the reader-tag distance. The EH output current could be used to recharge the battery during the system sleep time, by adding a low-power step up regulator. Up to 5 mm distance between the reader and the RFID tag, the output power (about 9.5 mW) is maximized with a 1 k $\Omega$  load and it is independent on the distance itself. It has been estimated that the supplied current by the EEPROM Energy Harvesting function during the 55 s sleep time could double the battery lifetime (130 h).

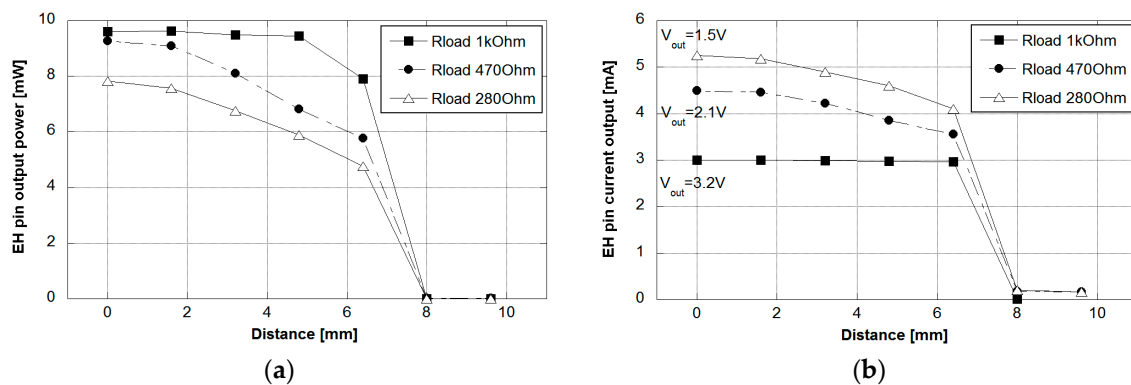


**Figure 11.** Electrically Erasable Programmable Read-Only Memory energy harvesting characterization as a function of the distance from the reader; in terms of power (a) and current (b); power can be extracted up to 6.5 mm distance.

#### 4. Conclusions

This paper described the development, the laboratory characterization, and preliminary in-vivo results of a potentially implantable blood pressure-sensing platform with an RFID interface. It shows a meaningful use of RFID interface to measure the vital signals. The electronic system exhibits performances and functionalities that make it suitable for implantable blood pressure telemetry. Two different pressure sensors were characterized, the first providing a digital output and the second an analog one. The system configuration with the digital pressure sensor produced the best performances in terms of power consumption (1.35 mA average current, 3.7 V supply) and resolution (0.4 mmHg<sub>rms</sub>). The in-vivo measurement, conducted implanting the catheter and not the electronics, provides results in accordance within 1 mmHg with those obtained with a reference sensor. Finally, a characterization of the Energy Harvesting function provided by the EEPROM with RFID interface has demonstrated the possibility to double the battery lifetime. The system exhibits volume, dimensions, and weight comparable with small-animals state-of-the-art telemetry systems, introducing some new features as the embedded processing, low cost PCB RFID antenna and energy harvesting functionality. In particular, the system is able to measure the pressure wave and, after embedded processing, to store the calculated blood pressure values onboard. Such data are available for subsequent interrogation by an external RFID reader. Nevertheless, the connection between the pressure sensor and the catheter is still to be optimized. As a consequence, the device is presently suitable for medium-size animals; the work is presently focusing on further tag miniaturization, achievable by choosing smaller packages for the electronics components, and on the biocompatible device encapsulation. Moreover, further long-term animal studies are planned to be performed in order to fully validate the system. It is worth emphasizing that the developed pressure sensing system is fitting for many applications, such as environmental or structural monitoring and human telemetry.

**Author Contributions:** V.R. and M.C. conceived and designed the experiments; B.N. performed the experiments; B.N. and M.C. analyzed the data; B.B. contributed to in-vivo tests; B.N. and M.C. wrote the paper.

**Conflicts of Interest:** The authors declare no conflict of interest.

#### References

1. Braga, V.A.; Burmeister, M. Applications of Telemetry in Small Laboratory Animals for Studying Cardiovascular Diseases. In *Modern Telemetry*; InTech: Rijeka, Croatia, 2011.
2. Rey, M.; Weber, E.W.; Hess, P.D. Simultaneous pulmonary and systemic blood pressure and ECG interval measurement in conscious, freely moving rats. *J. Am. Assoc. Lab. Anim. Sci.* **2012**, *51*, 231–238. [[PubMed](#)]

3. Romain, O.; Mazeyrat, J.; Garda, P.; Talleb, H.; Lautru, D.; Wong, M.-F.; Wiart, J.; Hanna, V.F.; Lagrée, P.-Y.; Bonneau, M.; et al. ENDOCOM: Implantable wireless pressure sensor for the follow-up of abdominal aortic aneurysm stented. *IRBM* **2011**, *32*, 163–168.
4. Todd, B.S.; Andrews, D.C. The identification of peaks in physiological signal. *Comput. Biomed. Res.* **1998**, *32*, 322–335. [[CrossRef](#)] [[PubMed](#)]
5. *Identification Cards—Contactless Integrated Circuit Cards—Vicinity Cards—Part 2: Air Interface and Initialization*; ISO/IEC 15693-2; International Organization for Standardization: Geneva, Switzerland.
6. *Identification Cards—Contactless Integrated Circuit(s) Cards—Vicinity Cards—Part 3: Anti-Collision and Transmission Protocol*; ISO/IEC 15693-3; International Organization for Standardization: Geneva, Switzerland.
7. Valdastri, P.; Menciassi, A.; Dario, P. Transmission power requirements for novel Zigbee implants in the gastrointestinal tract. *IEEE Trans. Biomed. Eng.* **2008**, *55*, 1705–1710. [[CrossRef](#)] [[PubMed](#)]
8. Aubert, H. RFID technology for human implant devices. *C. R. Phys.* **2011**, *12*, 675–683. [[CrossRef](#)]
9. Zhao, J. A new calculation for designing multilayer planar spiral inductors. *EDN (Electr. Des. News)* **2010**, *55*, 37–40.
10. Caldara, M.; Nodari, B.; Re, V. Development of a potentially implantable pressure sensing platform with RFID interface. In Proceedings of the 2013 IEEE Sensors, Baltimore, MD, USA, 3–6 November 2013.



© 2016 by the authors; licensee MDPI, Basel, Switzerland. This article is an open access article distributed under the terms and conditions of the Creative Commons Attribution (CC-BY) license (<http://creativecommons.org/licenses/by/4.0/>).